

## ON THE ACCURACY OF POLYNOMIAL FINITE ELEMENTS FOR CRACK PROBLEMS

A. R. JOHNSON

*Aero-Mechanical Engineering Laboratory, U.S. Army Natick Research and Development Command, Natick, MA,  
U.S.A.*

### SUMMARY

A square tensile sheet with symmetric edge cracks is analysed by the finite element method to demonstrate the accuracy obtained with polynomial elements when the mesh patterns are chosen on the basis of the element's interpolation functions. Numerical results are provided for the accuracy of the total strain energy, the stress intensity factor, and the numerical condition of the global stiffness matrix. The stress intensity factor is determined to within 1.0 per cent accuracy using quadratic (linear strain) triangular elements with only 138 degrees-of-freedom.

### INTRODUCTION

A great deal of effort has gone into the analysis of crack problems by the finite element method. Very accurate results can be obtained using hybrid elements, power law elements and 'quarter point' elements.<sup>1,2,3</sup> However, theoretical work indicates that if the displacement singularity is of the form  $R^\alpha$  with  $0 < \alpha < 1$  near the crack tip then the mesh near the crack tip can be designed to efficiently interpolate the power form of the displacement field in the energy norm.<sup>4</sup>

In this paper a square tensile sheet with symmetric edge cracks is analysed by the finite element method. The purpose of the analysis is to demonstrate the accuracy obtained when mesh patterns are chosen on the basis of the finite element's interpolation functions. A uniform mesh is used except in the immediate neighbourhood of the crack tip. Near the crack tip the element diameters are chosen so that the error per element in the energy norm is approximately equal for all elements. Using this technique the total strain energy and the stress intensity factor are determined to within 1.0 per cent accuracy when linear strain triangular elements are used with only 138 degrees-of-freedom. The ratio of the largest eigenvalue of the global stiffness matrix to the smallest (the condition number) is determined for each mesh pattern used. It is found that the nonuniform mesh patterns used here have small condition numbers.

### ANALYSIS OF SQUARE TENSILE SHEET

The geometry of the square tensile sheet with symmetric edge cracks analysed here is shown in Figure 1. The material is assumed to be linear with a modulus  $E = 1.0$ , Poisson's ratio  $\nu = 0.3$ , and a shear modulus  $G = E/(2(1+\nu))$ . When the region of concern is limited to the crack tip then with  $u, v =$  the material displacements in the  $x, y$  directions, respectively, the

0029-5981/81/121835-08\$01.00

© 1981 by John Wiley & Sons, Ltd.

Received 15 September 1980

Revised 29 December 1980

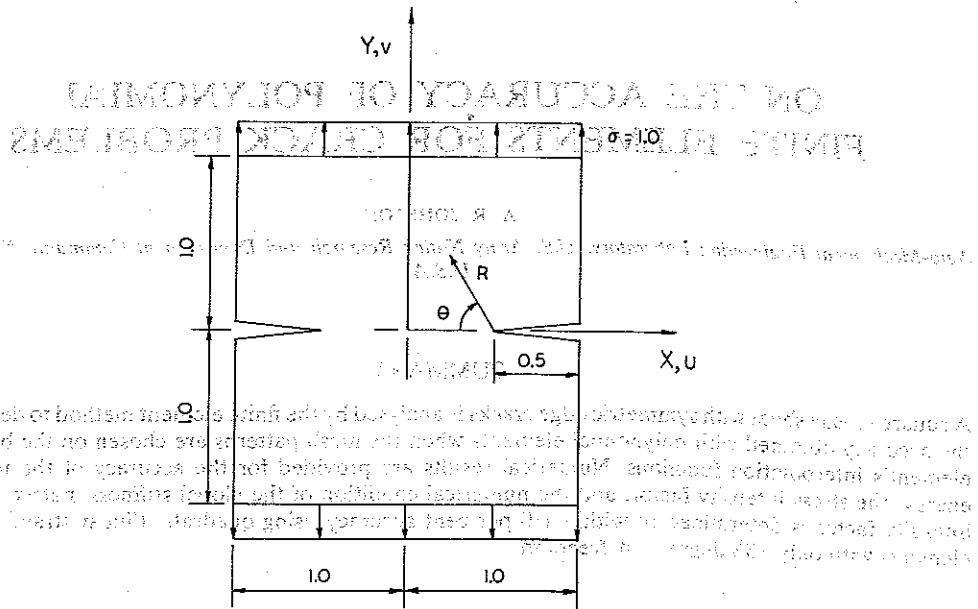


Figure 1. Square tensile sheet with symmetric edge cracks

near tip solution for mode 1 crack opening takes the following well-known asymptotic form:

$$u = \frac{K_1}{G} \sqrt{\frac{R}{2\pi}} \left( \cos \frac{\theta}{2} \left( (1-2\nu) + \sin^2 \frac{\theta}{2} \right) + O(R^{1/2}) \right)$$

$$v = \frac{K_1}{G} \sqrt{\frac{R}{2\pi}} \left( \sin \frac{\theta}{2} \left( (2-2\nu) - \cos^2 \frac{\theta}{2} \right) + O(R^{1/2}) \right)$$

where  $K_1$  is the stress intensity factor.

The equilibrium equations for plane strain assumptions in Cartesian co-ordinates can be written in the following form:

$$(\lambda + G)e_{xx} + G\nabla^2 u + X = 0$$

$$(\lambda + G)e_{yy} + G\nabla^2 v + Y = 0$$

where

$$X, Y = \text{body forces}$$

$$e = u_{,x} + v_{,y}$$

and

$$\lambda = \frac{\nu E}{(1+\nu)(1-2\nu)}$$

These equations are elliptic and the principal operators are of the form  $\nabla^{2m}$  with  $m = 1$ .

In 1972 Fried and Yang<sup>4</sup> developed a method for constructing mesh patterns for boundary value problems of the  $2m$ th order when the solution contains a singularity of the form  $R^\alpha$ , where  $0 < \alpha < 1$ . Their method determines a mesh pattern in which the energy error per

element is equally distributed among all the elements. In particular they demonstrated that for boundary value problems of order  $2m$  ( $m = 1$  for harmonic and  $m = 2$  for biharmonic) with displacement fields near the singular point of the form  $u = R^\alpha$ ,  $0 < \alpha < 1$ , the finite elements near the singularity should have their diameters chosen as follows:

$$d, \alpha_2 d, \alpha_3 d, \dots \quad (3)$$

where

$$\alpha_i = i^z$$

$$z = (2(p - \alpha) + 3 - n) / (2(\alpha - m) + n)$$

and where  $p$  is the order of the polynomial interpolation in the element,  $d$  the diameter of an element with one node at the singular point,  $m$  the order of the boundary value problem,  $n$  the number of dimensions in the boundary value problem, and  $\alpha$  the fraction describing the leading term in the displacement field singularity.

The square tensile sheet represents a two-dimensional boundary value problem,  $n = 2$ . The form of the singularity is given in equation (1),  $\alpha = 1/2$ , and the order of the boundary value problem is given in equation (2),  $m = 1$ . Thus, near the crack tip the element diameters should vary as indicated in Table I.

Table I. Near tip element diameters

Element interpolation functions (element type)	Near tip element diameters
Linear, $p = 1$ (constant strain triangles)	$d, 4d, 9d, \dots$
Quadratic, $p = 2$ (linear strain triangles)	$d, 16d, 81d, \dots$

Next, we develop finite element mesh patterns in which the element diameters are varied according to Table I and then we numerically determine the accuracy obtained when these mesh patterns are used. We will not construct a nonuniform mesh for the entire domain. Only the portion of the mesh near the crack tip will be nonuniform. These mesh patterns, although not optimum, can be easily constructed by anyone using a general-purpose finite element program. Figure 2 shows the construction of the finite element model. The maximum element diameter indicated in Figure 2 is the element diameter associated with a uniform mesh. The mesh near the crack tip was constructed as shown in Figure 3 with element diameter ratios as indicated in Table I.

The stress intensity factor,  $K_1$ , can be determined from the finite element data by a number of methods. Two methods were used here. The first method is called the extrapolation or tangent method. This method uses the displacement data,  $v$  vs  $R$ , and requires that

$$\lim_{R \rightarrow 0} (v/\sqrt{R}) \quad (4)$$

be determined from the data. Equation (1) is then used to determine  $K_1$ . Since the nodal data nearest the crack tip is the least accurate when polynomial elements are used, the data at the second and third nodes away from the crack tip was used here. The second method used here

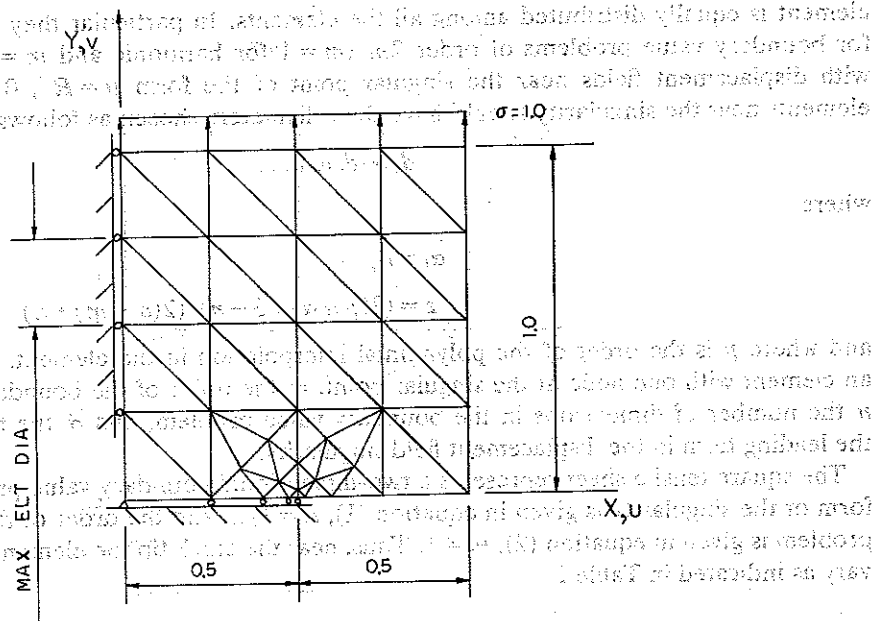


Figure 2. Typical finite element model.

to obtain  $K_1$  is called the energy release method. This method requires that the rate of change of the strain energy with respect to a change in the crack length,  $dU/da$ , be determined. Then,  $K_1$  is found from

$$-\left. \frac{dU}{da} \right|_{\text{load}} = \frac{1-\nu^2}{E} K_1^2 \quad (5)$$

To obtain a value for  $\left. \frac{dU}{da} \right|_{\text{load}}$  a second problem is solved with a different crack length. In

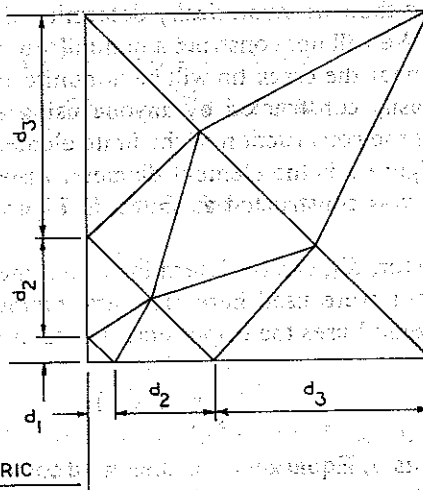


Figure 3. Mesh pattern near crack tip.

these calculations the second crack problem was defined by constraining one additional element on the  $x$ -axis from vertical displacements (see Figure 2).

To determine the relative error in the total strain energy and in the stress intensity factor their numerical values are required. In 1973 Tong and Pian<sup>5</sup> studied the convergence of finite element solutions for the square tensile sheet with edge cracks. Their calculations indicated that the total strain energy for the problem shown in Figure 1 is  $U = 3.228$ . In 1964 Bowie<sup>6</sup> analysed the rectangular tensile sheet with symmetric edge cracks using complex variable techniques. Using Bowie's results the stress intensity factor for the square tensile sheet analysed here is  $K_I = 1.61$ .

The numerical results obtained here, Tables II and III, are surprisingly accurate when the degrees-of-freedom, the types of elements, and the simplicity of the model construction are considered. When linear elements (constraint strain triangles) were used the stress intensity factor was obtained via the tangent method to within 2 per cent of the exact value with less than 200 degrees-of-freedom in the finite element model. When the quadratic elements (linear strain triangles) were used the stress intensity factor was accurate to three digits when only 138 degrees-of-freedom were used. The stress intensity factors determined by the tangent method were more accurate than those determined by the energy release method.

The finite element approximation  $\hat{U}$  of the strain energy converges to the exact value  $U$  as the number of elements is increased. Here the number of elements was increased by

Table II. Data for linear elements,  $p = 1$  (constant strain triangles)

Maximum element diameter		1/4	1/6	1/8
Degrees-of-freedom		74	122	186
Strain energy	value	3.01	3.08	3.11
	% error	6.7	4.7	5.5
$K_I$ (Tangent method)	value	1.53	1.58	1.59
	% error	5.0	1.9	1.2
$K_I$ (Energy method)	value	1.38	1.40	1.41
	% error	14.3	13.0	12.4

Table III. Data for quadratic elements,  $p = 2$  (linear strain triangles)

Maximum element diameter		1/2	1/4	1/6
Degrees-of-freedom		138	250	426
Strain energy	value	3.19	3.21	3.22
	% error	1.3	0.6	0.4
$K_I$ (Tangent method)	value	1.61	1.62	1.62
	% error	0.0	0.6	0.6
$K_I$ (Energy method)	value	1.55	1.56	1.56
	% error	3.7	3.1	3.1

uniformly reducing the maximum element diameter indicated in Figure 2. In this case the convergence can be approximated by the following power law:

$$\frac{\delta U}{U} = \frac{U - \hat{U}}{U} = C_0 N_e^p \quad (6)$$

where  $N_e$  are the total number of elements, and  $C_0, p$  are constants.

Figure 4 indicates that for the mesh patterns considered here the quadratic elements were more accurate and attained a higher convergence rate than the linear elements. If several nonuniform mesh patterns had been constructed for the entire domain of the square tensile sheet, Reference 4 indicates that even better results can be expected.

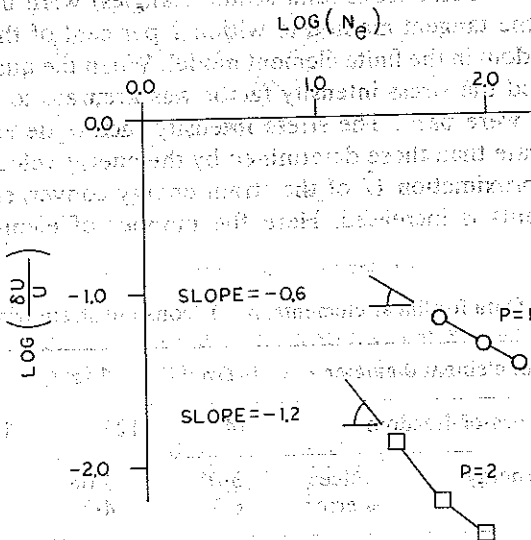


Figure 4. Strain energy accuracy vs. number of elements

The numerical condition number of an optimally scaled global stiffness matrix is related to the round-off errors in the finite element solution.<sup>7,8</sup> If the finite element system to be solved is  $Kx = b$  then the relative error in  $x$  is given as follows:

$$\frac{\|\delta x\|}{\|x\|} = 10^{-s} \min_{D} C(DKD) \quad (7)$$

where  $C$  is the ratio of the maximum eigenvalue of  $DKD$  to the minimum,  $D$  is a diagonal scaling matrix, and  $s$  is the number of digits in the computer words. In Reference 7 it was shown that

$$C(DKD) = C_1 \left( \frac{h_{max}}{h_{min}} \right)^{2m-1} (N_e)^{2m/n} \quad (8)$$

where  $h_{max}$  and  $h_{min}$  are the maximum and minimum distances between nodal points,  $m$  is the order of the boundary value problem,  $n$  the number of physical dimensions,  $N_e$  the number of elements, and  $C_1$  is a constant. In these calculations the ratio of  $(h_{max}/h_{min})$  is 1/14 for the linear elements and 1/98 for the quadratic elements,  $m = 1$ , and  $n = 2$ . Here, we have

$(h_{\max}/h_{\min}) = \text{a constant for each type of element. Thus equation (8) yields}$

$$C(\mathbf{DKD}) = O(N_e) \quad (9)$$

In Reference 8 the condition of a two-dimensional second-order circular membrane problem discretized by a nonuniform mesh of linear triangular elements is determined. Upper and lower bounds for the condition numbers are determined. For that problem it is shown that the condition number is more sensitive to the minimum angle in an element than it is to the ratio of the largest to smallest element diameters. When the mesh is refined as suggested here (maximum mesh ratio and minimum angle in an element both remaining constant) the upper bound on the condition number in Reference 8 also reduces to equation (9), above.

A practical scaling technique was developed by Lanczos.<sup>9</sup> This technique scales the matrix  $\mathbf{K}$  so that the terms in each row of  $\mathbf{DKD}$  on the diagonal are of value 1.0. Using this scaling technique the condition number of the scaled stiffness matrix is shown in Figure 5 for both

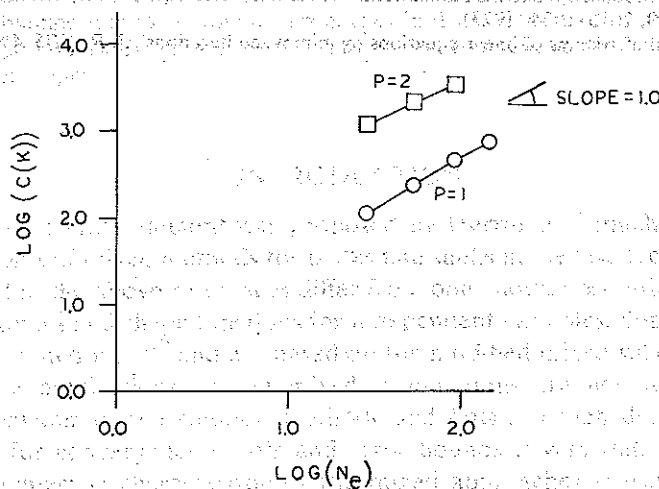


Figure 5. Condition of global stiffness matrix vs. number of elements

linear and quadratic elements. The results indicate that for practical mesh patterns ( $N_e < 150$ ) the condition numbers are small enough so that the effects of round-off errors are not serious even in single precision calculations ( $s = 7$ ). Also, the theoretical growth rate of the condition number predicted in equation (9) is represented well in Figure 5.

#### CONCLUSION

A technique for designing finite element mesh patterns for elliptic boundary value problems that have solutions containing a power-type singularity has been numerically investigated for a crack problem in linear elasticity. Using only polynomial finite elements and restricting the nonuniform mesh to the immediate crack tip region, useful values of the strain energy and stress intensity factors were obtained with relatively few degrees-of-freedom. The element diameter ratios used were not large (14/1 for the linear elements and 98/1 for quadratic). The resulting global stiffness matrix was well conditioned and the theoretical asymptotic growth rate of the condition number was observed.

ACKNOWLEDGEMENT: This research was supported by ILIR Project A91A, Department of the Army, U.S.A.

This research was supported by ILIR Project A91A, Department of the Army, U.S.A.

REFERENCES

1. P. Tong, T. H. H. Pian and S. J. Lasry, 'A hybrid-element approach to crack problems in plane elasticity', *Int. J. num. Meth. Engng*, **7**, 297-308 (1973).
2. D. Tracey and T. Cook, 'Analysis of power type singularities using finite elements', *Int. J. num. Meth. Engng*, **11**, 1225-1233 (1977).
3. Y. Yamada, Y. Ezawa, I. Nishiguchi and M. Okabe, 'Reconsiderations on singularity or crack tip elements', *Int. J. num. Meth. Eng.*, **14**, 1525-1544 (1979).
4. I. Fried and S. K. Yang, 'Best finite elements distribution around a singularity', *A.I.A.A. J.*, **10**, 1244-1246 (1972).
5. P. Tong and T. H. H. Pian, 'On the convergence of the finite element method for problems with singularity', *Int. J. Solids Struct.*, **9**, 313-321 (1973).
6. O. L. Bowie, 'Rectangular tensile sheet with symmetric edge cracks', *J. Appl. Mech.*, **31**, 208-212 (1964).
7. I. Fried, 'Condition of finite element matrices generated from nonuniform meshes', *A.I.A.A. J.*, **10**, 219-221 (1972).
8. I. Fried, 'Bounds on the spectral and maximum norms of the finite element stiffness, flexibility and mass matrices', *Int. J. Solids Struct.*, **9**, 1013-1034 (1973).
9. C. Lanczos, 'Solution of systems of linear equations by minimized iterations', *J. R. NBS*, **49**, 33-53 (1952).

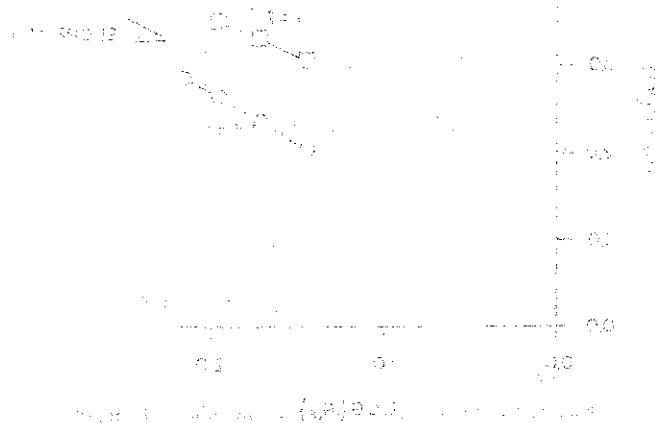


Figure 1. A plot of the function  $y = \sqrt{x}$  for  $x$  in the range [0, 1]. The x-axis is labeled from 0 to 1.0, and the y-axis is labeled from 0.0 to 1.0. The curve starts at the origin (0,0) and increases as it moves towards the top right, passing through approximately (0.2, 0.4) and (0.4, 0.6).

The figure shows a plot of the function  $y = \sqrt{x}$  for  $x$  in the range [0, 1]. The x-axis is labeled from 0 to 1.0, and the y-axis is labeled from 0.0 to 1.0. The curve starts at the origin (0,0) and increases as it moves towards the top right, passing through approximately (0.2, 0.4) and (0.4, 0.6). This curve represents the square root function, which is a common example of a function with a singularity at the origin.